# Gyrokinetic Simulation of Dissipative Trapped Electron Mode in Tokamak Edge

C. Zhao, Y. Xiao*

Inst. Fusion Theory and Simulation, ZhejiangUniv., Hangzhou 310027, China

* (Corresponding author) Email: yxiao@zju.edu.cn

1/27/2017

The gyrokinetic simulation using GTC is carried out for the dissipative trapped electron mode (DTEM), which is an important source for the electrostatic turbulence in the pedestal of tokamak plasmas. The DTEM instability is identified for the edge plasmas and its dependence on the wavelength and collisional frequency is obtained by both simulation and theory. It is shown for the first time that the linear gyrokinetic simulation results are fully consistent with that from the analytic theory under the edge parameters. This suggests that the GTC code can simulate accurately the DTEM instability in the pedestal. It provides a useful benchmark for gyrokinetic simulations of the edge plasmas.

## I Introduction

Low frequency drift-wave turbulence induced by plasma pressure gradient is an important candidate for anomalous transport in tokamaks. In particular, turbulence driven by trapped electron instabilities, namely collisionless trapped electron mode (CTEM) and dissipative trapped electron mode (DTEM), can be responsible for the radial electron transport in tokamak plasmas. The CTEM, excited by precessional resonance of the magnetically trapped electrons, has been extensively investigated by theory [1][2] and gyrokinetic simulation [3][4][5]. Many physics understandings of the DTEM have been gained, in particular its linear instability threshold, nonlinear saturation, and transport characteristics. On the other hand, the DTEM in the tokamak pedestal region is less well understood [6]. Using a simple Krook collision operator, Cheng et. al. presented a linear theory of DTEM for the instability condition and two dimensional mode structures [7]. Recently, interest on the DTEM has been revived by the observation of the so called edge coherent mode observed in the EAST experiments [8]. In the H-mode regime, the DTEM can play an important role in the pedestal region since (1) the population of the trapped electrons increases with radius and maximize near the plasma edge, (2) the edge plasma temperature drops fast and becomes so low that the collisions can not be ignored, and (3) the pressure profile is so steep that the resonant interaction between the drift waves and the trapped electrons is rather weak. In this work, we use the gyrokinetic code GTC [9] to investigate the linear physics of DTEM in the tokamak pedestal. For the first time the pedestal DTEM simulations are fully consistent with the analytical theory that includes the pitch angle scattering collisions. This suggests that the GTC code can simulate accurately the DTEM instability for tokamak edge plasmas. Accordingly, the GTC code should be useful for simulating the DTEM turbulence at the tokamak edge, where the plasma has sharp gradients and collisions are important. In addition, this work provides an ideal example to benchmark the capability of the gyrokinetic code in simulating the DTEM instability in the tokamak edge.

This paper is organized as follows. In Sec. II we discuss the simulation model and parameters. Then the results for the DTEM obtained from the GTC simulation are presented, and compared with an analytic theory in Sec. III. The analytical theory is given in detail in Sec. IV. Finally the discussions and conclusions are given in Sec. V.

# II Simulation model and parameters

The GTC code is a three-dimensional global gyrokinetic particle code using the Boozer coordinates for general magnetic field geometry in tokamaks [9]. It invokes a nonlinear $\delta f$ scheme [10] for investigating waves and instabilities, turbulence, neoclassical transport and other important physics in tokamaks [11][12]. The GTC code has low particle noise due to the use of the $\delta f$ scheme and a field-aligned mesh. The implementations of a gyrokinetic Poisson solver [13] suitable for general magnetic field geometry and guiding center equations of motion [14] in magnetic coordinates [15] enable the code to efficiently simulate phenomena in many magnetic confinement devices using realistic numerical plasma equilibria. The code is truly global as it solves the gyrokinetic Poisson equation in real space and has the unique capability to simulate a full poloidal cross section using zero radial boundary conditions. It has been rigorously benchmarked against the existing analytic theories and other gyrokinetic simulations for important issues such as neoclassical transport [16] and turbulent transport [13][17]. In particular, the linear frequency and growth rate of the ion temperature gradient (ITG) mode and collisionless trapped electron mode (CTEM) have been shown to agree well with other codes for the tokamak core plasmas [18].

In the GTC simulation, the particle distribution is decomposed into an equilibrium Maxwellian distribution $F_0$ and a perturbed distribution function $\delta f$. The latter one for ions, i.e. $\delta f_i$, is given by the gyrokinetic equation:

$$\left[\frac{\partial}{\partial t}+\left(v_{\|}\hat{b}+\mathbf{v}_d\right)\cdot\nabla\right]\delta f_i=-\left(\mathbf{v}_E\cdot\kappa_{pi}+\frac{Z_i e}{T_i}v_{\|}E_{\|}-\frac{Z_i e}{T_i}\mathbf{v}_d\cdot\nabla\delta\phi\right)F_{0i}, \tag{1}$$

where $Z_i$ is the ion charge number, $\mathbf{v}_d=\mathbf{v}_g+\mathbf{v}_c=v_{\|}^2\nabla\times\hat{b}/\omega_{ci}+\mu\hat{b}\times\nabla B_0/(m\omega_{ci})$ is the $\nabla B$ and curvature drift velocity, $\mathbf{v}_E=c\hat{b}\times\nabla\delta\phi/B_0$ is the $E\times B$ drift velocity,

$\hat{b} \equiv \mathbf{B}_0 / B_0$ is the unit vector along the field line, $\omega_{ci} = Z_i eB_0 / m_i c$ is the ion cyclone frequency, $\kappa_{ps} \equiv \nabla \ln n_0 + \left[ m_s v^2 / (2T_s) - 3/2 \right] \nabla \ln T_s$ with $s = i, e$ represents the ion or electron pressure gradient.

The perturbed electron distribution $\delta f_e$ consists of an adiabatic response $\delta f_e^{(0)} = e\delta\phi F_0 / T_e$ and non-adiabatic response $\delta g_e$ that satisfies the drift kinetic equation:

$$\left[ \frac{\partial}{\partial t} + \left( v_\parallel \hat{b} + \mathbf{v}_d \right) \cdot \nabla - C_{ei} \right] \delta g_e = -F_{0e} \left[ \mathbf{v}_E \cdot \nabla \ln F_{0e} + \frac{\partial}{\partial t} \left( \frac{e\delta\phi}{T_e} \right) - \mathbf{v}_d \cdot \nabla \left( \frac{e\delta\phi}{T_e} \right) \right]. \tag{2}$$

The $\delta f$ method used in the GTC efficiently limits the Monte Carlo noise associated with the numerical particles. We denote $w_i = \delta f_i / f_i$, $w_e = \delta f_e / f_e$, so that one can write

$$\frac{d}{dt} w_i = -(\mathbf{v}_E \cdot \kappa_{pi} + \frac{Z_i e}{T_i} v_\parallel E_\parallel - \frac{Z_i e}{T_i} \mathbf{v}_d \cdot \nabla \delta\phi), \tag{3}$$

$$\frac{d}{dt} w_e = -\left[ \mathbf{v}_E \cdot \kappa_{pe} - \frac{e}{T_e} \mathbf{v}_d \cdot \nabla \delta\phi + \frac{\partial}{\partial t} \left( \frac{e\delta\phi}{T_e} \right) \right], \tag{4}$$

The collisions on the electrons are dominated by the electron-ion collisions, which can be represented for simplicity by a pitch angle scattering operator, given by the following Monte-Carlo process [19][20]:

$$\xi_{t+\Delta t} = \xi_t \left( 1 - \nu_{ei} \Delta t \right) + \left( R_n - 0.5 \right) \sqrt{12 \left( 1 - \xi_n^2 \right) \nu_{ei} \Delta t}. \tag{5}$$

where $\xi = v_\parallel / v$ is the pitch angle of the particle motion, $\Delta t$ is the time step, and $R$ is a random number uniformly distributed between 0 and 1.

For simplicity, we shall assume concircular flux surfaces. The tokamak edge parameters are $R_0/L_{Ti}=69.2$, $R_0/L_{Te}=69.2$, $R_0 L_n=69.2$, $m_i/m_e=1837$, $q=0.85+1.10r/a+1.00(r/a)^2$, $\varepsilon=0.3$, $\mathrm{n}=26$, where $L_{Ts}=1/\partial_r \ln T_s$ with $s=i,e$ is the scale length of the temperature gradient, $L_n=1/\partial_r \ln n$ is the scale length of the density gradient, $\varepsilon=a/R_0$ with $R_0$ the major radius of the tokamak, $a$ is the minor radius of the tokamak, and $r$ is the radial coordinate. The toroidal magnetic field is defined by $B_T=B_0/[1+(r/a)\cos(\theta)]$, with $\theta$ the poloidal angle. The mesh for the electromagnetic field perturbations consists of 32 or 64 grids in the parallel or toroidal direction, and hundreds of grids in the poloidal direction on each flux surface. An unstructured poloidal mesh is used with grid size about $0.5\rho_\mathrm{i}$ or $1.0\rho_\mathrm{i}$ in the radial or poloidal directions to simulate the short perpendicular-wavelength modes.

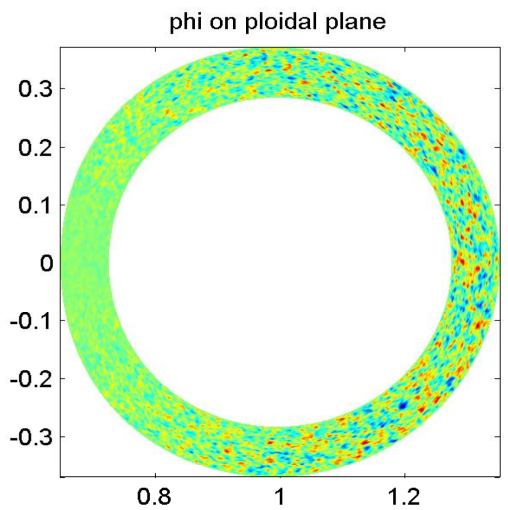


(a)

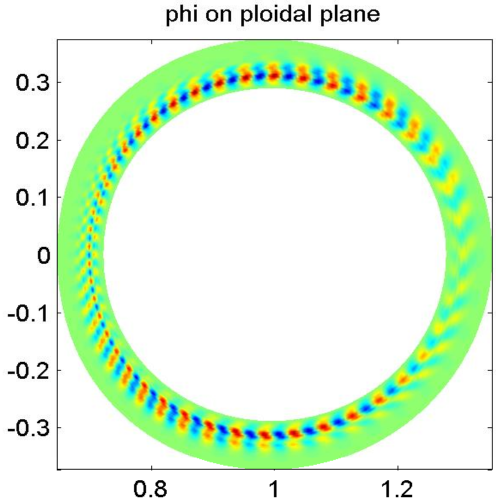


(b)

Figure 1: Electrostatic potential on the poloidal plane for $\nu_e^* = 0$ (a) and $\nu_e^* = 0.2$ (b).

# III Gyrokinetic simulation results for edge DTEM

Figs. 1(a) and (b) show the electrostatic potential on the poloidal plane for plasma without collisions and with collisions, respectively. For the collisional case, the effective collisional frequency is $\nu_e^* = 0.2$, with $\nu_e^* = \nu_{Te} q R_0 \big/ \left( v_{Te} \varepsilon^{3/2} \right)$ where $\nu_{Te} = n_i Z_i^2 e^4 \big/ \left( 4\pi\varepsilon_0^2 m_e^2 v_{Te}^3 \right)$, $\varepsilon_0$ is the dielectric constant of the vacuum. As can be seen in Fig. 1(a), in the collisionless case there is no unstable mode. However, Fig. 1(b) indicates that in the collisional case an unstable DTEM mode is excited. The latter can be attributed to collisional detrapping of some magnetically trapped electrons. It is also found that the most unstable region is not that (around θ = 0) having the worst curvature. This unusual mode structure can be attributed to the strong pressure gradient in the pedestal region, where the magnetic drift frequency is much smaller than the diamagnetic frequency [21].

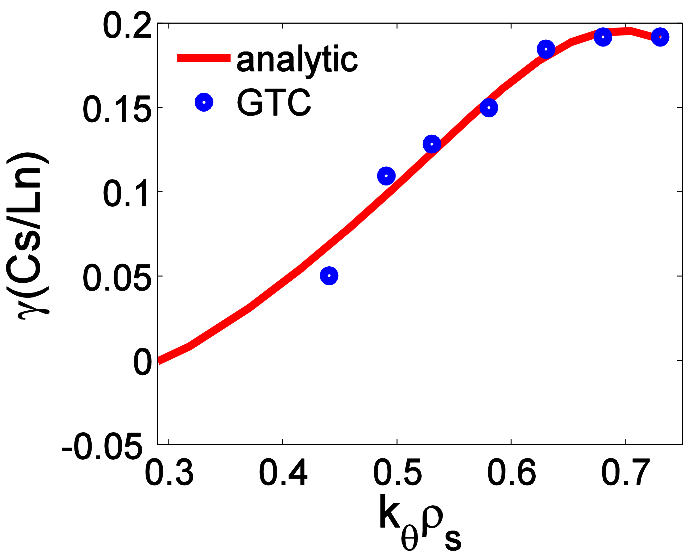


(a)

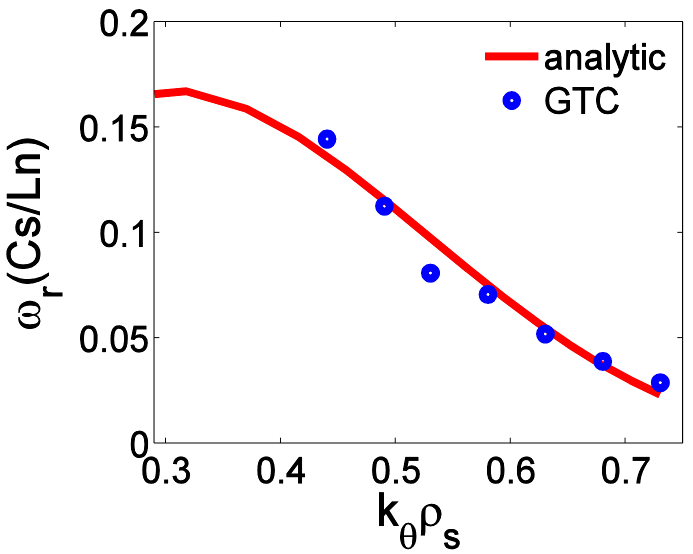


(b)

Figure 2: Linear growth rate (a) and real frequency (b) vs. $k_\theta \rho_s$ for $\nu_e^* = 0.2$.

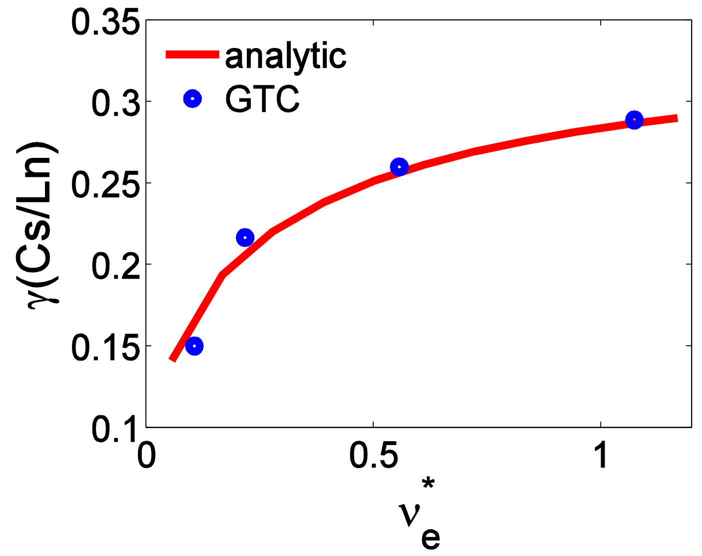


Figure 3: Linear growth rate vs. $\nu_e^*$.

Fig. 2 shows the dependence of the linear growth rate and real frequency on the poloidal wavelength. The solid curve is from the analytical theory given in Sec. IV, and the open circles are from our GTC simulation. One can see that the GTC results are fully consistent with that from the theory and the short-wavelength modes have higher growth rates than the long-wavelength modes. In Fig. 3 we see that the growth rate increases with the effective collision frequency for $\nu_e^* < 1$. Under the given parameters, the real frequency of the DTEM is $\omega_r \sim 0.1 C_s / L_n$, which is roughly independent of the collisional frequency and consistent with the theory given in the following section.

# IV DTEM theory for tokamak edge

The theoretical results presented in Figs. 2 and 3 are from a gyrokinetic theory applied to the pedestal region [22], where one assumes that $\omega \sim \omega^* >> \omega_d$, $\nu_{ei} << \omega_b$. For convenience, the particle distribution function is expressed as

$$f_s = F_{0s} - \frac{e_s \delta\phi}{T_s} F_{0s} + \delta H_s e^{ik_\perp \rho_{Ls}} \tag{6}$$

where $F_{0s}$ is the equilibrium distribution function with $s = i, e$ for ions and electrons respectively, $-e_s \delta\phi F_{0s} / T_s$ is the adiabatic part of the perturbed distribution function, $\delta H_s$ is the non-adiabatic or kinetic part of the perturbed distribution function, $k_\perp$ is the wave vector perpendicular to the static magnetic field, and $\rho_{Ls} = v_\perp / \omega_{cs}$ is the Larmor radius, and $\omega_{cs} = e_s B / m_s c$ is the gyro-frequency. In the long wavelength limit $k_\perp \lambda_e << 1$, the Poisson equation solved for the electrostatic field becomes the quasi-neutrality condition

$$\frac{n_0 e^2 \delta\phi}{T_e} \left(1 + Z_i^2 \tau\right) = \left\langle Z_i e J_0 \delta H_i \right\rangle - \left\langle e \delta H_e \right\rangle \tag{7}$$

where $J_0 = J_0\left(k_\perp \rho_i\right)$ is the zeroth order Bessel function, $\tau = T_e / T_i$, and $\langle \cdots \rangle$ denotes the integration over the velocity space. The collisions, parallel resonance and magnetic drifts for the ions can be neglected in the low frequency limit $\omega << k_\parallel v_{ti}$. Thus $\delta H_i$ has the following solution after simplifying the ion gyrokinetic equation

$$\delta H_i = -\frac{Z_i e}{T_e} \tau \left[ 1 + \frac{\omega_{*e}}{\omega} \left( 1 + \eta_i \left( \frac{m_i v^2}{2T_i} - \frac{3}{2} \right) \right) \right] F_{0i} J_0\left(k_\perp \rho_i\right) \delta\phi \tag{8}$$

where $\omega_{*e} = k_\theta T_e L_n c / eB$ is the electron diamagnetic frequency.

In tokamaks the electrons can be separated into passing and trapped electrons. Accordingly, it is convenient to define a pitch angle variable $\kappa \equiv [(1/2)v^2 - \mu B_0(1-\varepsilon)]/2\varepsilon\mu B_0$ for a large aspect ratio circular tokamak, such that $0 \le \kappa \le 1$ and $\kappa \ge 1$ correspond to the trapped and passing electrons, respectively. For the low frequency drift waves the response of the passing electrons remains adiabatic. However, the kinetic response of the trapped electrons must be calculated and can be obtained by averaging the electron drift kinetic equation over their bounce orbit. Moreover, in the steep pressure gradient region the magnetic drift can be ignored. For the electron-ion collisions, we use a pitch angle scattering or the Lorentz collision operator, which can also be bounce averaged. The electron distribution can then be obtained by solving the bounce averaged gyrokinetic equation [22]:

$$\delta H_{etr} = -\frac{e\delta\phi}{T_e} Q(v) F_{oe} \left[ 1 - \frac{J_0(2(1+i)\sqrt{\kappa/\nu_{eff}})}{J_0(2(1+i)\sqrt{1/\nu_{eff}})} \right] \tag{9}$$

$$\delta H_{ep} = 0 \tag{10}$$

where $\delta H_{etr}$ is the kinetic distribution function for the trapped electrons, $\delta H_{ep}$ is the kinetic distribution function for the passing electrons, $Q(v) = 1 - \omega_{*e}/\omega \times \left[1 + \eta_e \left(m_e v^2/(2T_e) - 1.5\right)\right]$, $\varepsilon$ is the inverse aspect ratio, $\nu_{eff} = \nu_e/\omega\varepsilon$, $\nu_e = n_e e^4 / 4\pi\varepsilon_0^2 m_e^2 v^3$, $\varepsilon_0$ is the dielectric constant of the vacuum.

Inserting the ion and electron responses in Eqs. (8)-(10) in the quasi-neutrality condition, i.e. Eq. (7), and treat the ion as proton , i.e. $Z_i = 1$, one obtains the following integral equation for the pedestal DTEM dispersion relation

$$\Omega-\frac{2\sqrt{2\varepsilon}}{\pi^{3/2}}\int_0^1 d\kappa K(\kappa)\int_0^\infty t^{\frac{1}{2}}e^{-t}\times\left(\frac{J_0(\sqrt{\kappa}x)}{J_0(x)}\right)\left\{\Omega-\left[1+\eta_e\left(t-\frac{3}{2}\right)\right]\right\}dt$$

$$+\Omega\tau-\left(\Omega\tau+1\right)\Gamma_0(b)+\eta_i b\left(\Gamma_0(b)-\Gamma_1(b)\right)=0, \qquad (11)$$

where $t=m_e v^2/2T_e$, $x=2(1+i)\big/\sqrt{\nu_{eff}}$, $\Omega=\omega/\omega_{*e}$, $b=(k_\perp\rho_i)^2\equiv k_\perp^2 T_i/m_i\omega_{ci}^2$, $\Gamma_n=I_n(b)e^{-b}$, $n=0,1,$ and $I_n$ is the *n*th order modified Bessel function. Instead of using the approximation given in Ref. 21, we can be more precise by numerically evaluating the integral on the left hand side of Eq. (11). Choosing the latter Eq. (11) then becomes an algebraic equation from which the eigenvalue $\Omega\equiv\Omega_r+i\Omega_i$ can be obtained. The results are shown in Fig. 4 for $\varepsilon=0.2,$ $\nu_e^*=0.1,0.5,1,$ $\tau=1,$ $\eta_i=\eta_e=1,$ $R_0/L_n=69.2$. We see that for $\nu_e^*=0.1$ the longer wavelength modes are stable, and as $\nu_e^*$ increases the stable region becomes smaller. Fig. 4 also shows that the growth rate increases with $k_\theta\rho_i$ while the real frequency decreases with $k_\theta\rho_i$. The unstable mode propagates in the electron diamagnetic direction since $\Omega_r>0$. One can see that $\Omega_r$ does not change much when $\nu_e^*$ increases from 0.1 to 1.0, confirming that the real frequency is mainly determined by the collisionless response of the electrons.

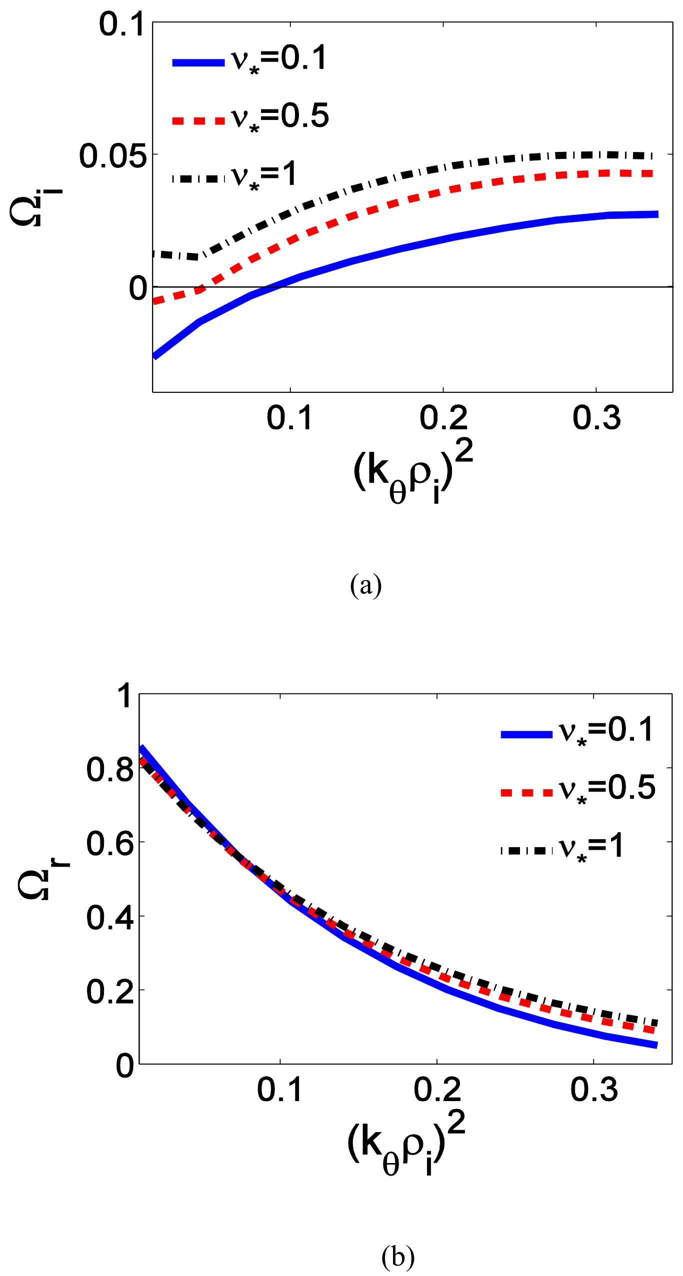


Figure 4: Theoretical linear growth rate and real frequency vs. $(k_\theta \rho_i)^2$ for different collisional frequencies.

# V Conclusion and discussion

In this paper we have used the GTC code to simulate the DTEM instability in the tokamak edge region. The gyrokinetic DTEM results are for the first time verified by an analytical theory for the edge region, which not only demonstrates that the GTC code can accurately simulate the DTEM instability, but also provides a useful benchmark for the DTEM simulation in the edge region, where the plasma density and temperature gradients are high and collisions are the dominant destabilizing factor. The analytical model numerically integrates the trapped electron response and gives a more accurate DTEM dispersion relation. Our results show that for $\nu_e^* < 1$, the electron-ion collisions can drive the DTEM instability, and the shorter-wavelength modes are easier to excite than the long-wavelength ones. For weak collisions, even the long-wavelength modes can be stable. With the linear DTEM fully verified, the gyrokinetic simulation using GTC is ready for investigating the interesting nonlinear physics in the tokamak pedestal.

## Acknowledgments

The work is supported by National Magnetic Confinement Fusion Energy Research Program under Grant No. 2015GB110000, 2013GB111000, China NSFC under Grant No. 11575158, the Recruitment Program of Global Youth Experts. We would thank Professor L. Chen, Z. Lin & M.Y. Yu for useful discussions.

## Bibliography

[1] J. Adam, W. Tang, and P. Rutherford, Phys. Fluids 19, 561(1976)

[2] P. J. Catto and K. T. Tsang, Physics of Fluids (1958-1988) 21, 1381 (1978).

[3] J. Lang, S. Parker, and Y. Chen, Phys. Plasmas 15, 055907(2008)

[4] G. Rewoldt, Z. Lin, and Y. Idomura, Comput. Phys. Commun. 177, 775 (2007)

[5] Y. Xiao and Z. Lin, Phys. Plasmas 18, 110703(2011).

[6] D. Ernst et al., Phys. Plasmas 11, 2637 (2004)

[7] C. Z. CHENG, L. CHEN, NUCLEAR FUSION, Vol.21, No.3 (1981).

[8] H.Q.Wang，G.S.Xuet al.,Phys. Rev. Lett. 112, 185004(2014)

[9] Z.Lin, T.S.Hahm, W.W.Lee, W.M.Tang, R.B.White, Physics of Plasmas (1994-present), 2000, 7(5):1857-1862.

[10] A.M.Dimits, W.W.Lee, Journal of Computational Physics, 1993, 107(2):309-323.

[11] Z. Lin,W. M. Tang, W. W. Lee, Phys. Plasmas, Vol. 2, No. 8, August (1995).

[12] Y.Xiao,Z.Lin, PRL 103, 085004 (2009).

[13] Y. Xiao, I. Holod, Z. X. Wang, Z. Lin, T. G. Zhang, Phys. Plasmas 22, 022516 (2015).

[14] R. B. White and M. S. Chance, Phys. Fluids 27, 2455 (1984).

[15] A. H. Boozer, Phys. Fluids 24, 1999 (1981).

[16] Z. Lin, W. M. Tang, and W. W. Lee, Phys. Rev. Lett. 78, 456 (1997).

[17] W. Deng, Z. Lin, I. Holod, Z. Wang, Y. Xiao, and H. Zhang, Nuclear Fusion 52, 043006 (2012).

[18] G. Rewoldt, Z. Lin, and Y. Idomura, Comput. Phys. Commun. 177, 775 (2007)

[19] Z. Lin and W. W. Lee, Phys. Rev. E 52, 5646 (1995).

[20] X. Q. Xu and M. N. Rosenbluth, Phys. Fluids B 3,627 (1991)

[21] H.S. Xie, **Y. Xiao**, PHYSICS OF PLASMAS 22, 090703 (2015)

[22] J.W.Connor, R.J.Hastie and P.Helander, Plasma Phys. Control. Fusion 48 (2006) 885 ̇C900.

[23] G. Rewoldt, W. M. Tang and E. A. Frieman, Phys. Fluids 20, 402 (1977).

[24] P. H. Rutherford,E. A. Frieman, Physics of Fluids (1958-1988) 11, 569 (1968).